Experimental Phased-Array Excitation Guided Utilizing a Computational Electromagnetic Model: Initial Findings

T. S. Ibrahim[1], Y-K. Hue[1], F. Boada[1], J. Nistler[2], J. Fontius[2], and F. Schmitt[2]

[1]University of Pittsburgh, Pittsburgh, Pennsylvania, United States, [2]Siemens Medical Systems

Introduction: Ultra high field imaging (1-4) and transmit (TX) SENSE (5) have accelerated the concept of variable phase/amplitude (RF shimming/phased array) excitation (6,7) into hardware development. This concept has tremendous potential for alleviating many of the severe B_1 field inhomogeneities associated with human high and ultra high field MRI. To harness the full potential of this technique however, phased array excitation/RF shimming, which requires knowledge of the electromagnetic fields produced by the phased-array-excited transmit arrays in the load, needs to be fully and automatically implemented in the experimental setting. To date, this important goal had remained elusive due to the lack of 1) appropriate hardware and 2) a method that can directly/accurately provide the phases and the amplitudes of the voltages exciting the transmit array prior to conducting the experiment. In this work, we present the first preliminary demonstration of prospective B_1 shimming based on full wave computational electromagnetics that simultaneously account for 1) interactions between the array elements and the load, 2) the coupling between the array elements, and 3) the array input impedance. The proposed method was successfully tested on a whole-body 3T scanner (Siemens Magnetom TRIO) A TIM system, equipped with an 8 channel phased-locked TX Array. We demonstrate that the proposed method can prospectively provide the phases/amplitudes of the voltages that should be applied to the coil elements in order to improve the homogeneity of the B_1 field.

Methods: An in-house computational electromagnetic modeling-system based on the finite difference time domain (FDTD) method was developed to fully model an-eight port transmit head coil previously utilized for transmit SENSE at 3 Tesla (8). Its diameter and length are 280mm and 200mm, respectively with two eight-set of tuning capacitors that are mounted on the front and back endrings, and 8 capacitors on each rung to facilitate the decoupling of the coil elements. The coaxial feeding lines are connected to the top ring of the coil. In the FDTD model, the 8-channel coil combined with a non-conventional (to FDTD) true eight-transmission lines feeding (9) were developed. The numerical tuning of the coil, similar to the experiment, is carried out to avoid cross-talk/coupling between excitation ports. While a minimum of 17 dBs (in the experiment and the FDTD model) was achieved for all of the ***S*** scattering parameters, the accumulate effects of the interactions/reflections/matching of the ports had to be considered and converted between the simulations and the experiment through a model/experiment transformation method. Additionally, to account for the effect of the physical imperfections of the experimental coil, the experimental ***S*** parameters of the system were utilized as part of the modeling system. The distributions of the B_1^+ field due to the eight ports were recorded at the frequency of interest (123MHz) and variable phase/amplitude driving scheme was implemented both numerically and experimentally at 3 Tesla.

Results/Discussion/Conclusions: *In the following results, the drive ports of the models are slightly shifted from the experimental ones.* Fig. 1 shows a low flip angle numerical (without including the experimental coupling adjustments) and experimental image of a one-port excited coil loaded with a 17-cm inner diameter sphere filled with saline (static conductivity = 1.15 S/m and dielectric constant = 79). While the rest (7) of the ports were not excited, they are present and inductively coupled. Fig. 2 depicts an anti-circular polarization excitation performed using the Siemens 8-channel phased-locked TX Array. Looking into the central region of the phantom, it can be clearly shown that without using the ***S*** parameters experimental adjustments, the simulated image is azimuthally symmetric because it represents the symmetrical coil and phantom positioning. Use of the ***S*** parameters adjustments (Fig. 2 middle), which are experimentally measured prior to imaging, leads to the simulated results that better match the experimental images (both of which are not azimuthally symmetric as denoted by the two dark minimums in the center of the phantom). Such arrangement can therefore be utilized to guide the phased array excitation even in an imperfect/asymmetric transmit array. To demonstrate the last point and underscore the importance of the scattering ***S*** parameters adjustments, Fig 3 depicts a three-port arbitrary/variable phase/amplitude excitation. While the simulated results closely match the experimental ones, the ***S*** parameters adjustments have smaller effect in this case since the three excited ports are relatively far from each other (at least one non-excited port is present between the excited ports). Thus, the coupling between the ports is weak and therefore ***S*** parameters adjustments may not be needed.

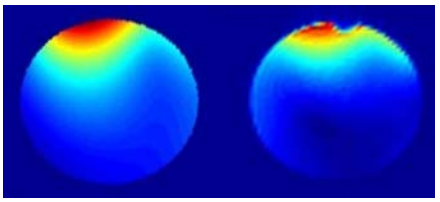

Fig. 1, Low flip angle image of 1-port excitation. Left image corresponds to the simulated results (without experimental coupling adjustments due to physical coil imperfections/coupling) while right image corresponds to the experimental result.

The preliminary results demonstrate that, with experimental/numerical ***S*** parameters adjustments done prior to imaging and a properly modeled load, variable phase/amplitude excitation can be efficiently optimized for any # of channels and can be guided through computational electromagnetics with only a minimum of computational time required (seconds). These developments can pave the way for a fully automatic, subject specific, B_1 homogenization/localization scheme for ultra-high field imaging.

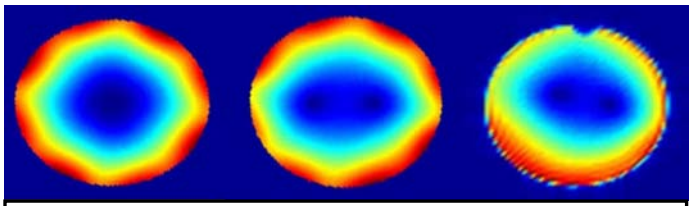

Fig. 2, Low flip angle image of an eight-port anti-circular polarization excitation. The left image is the simulated result without using the experimental/numerical ***S*** parameters adjustments; the center image is the simulated result using the experimental/numerical ***S*** parameters adjustments. The right image is the experimental result.

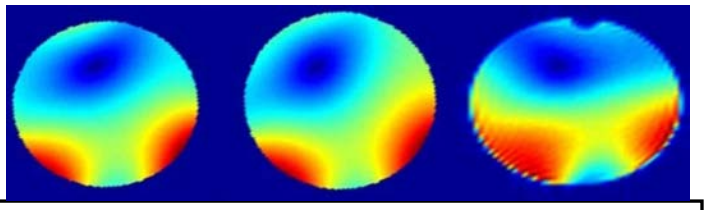

Fig. 3, Low flip angle image of a three-port arbitrary/variable phase/amplitude excitation. The left image is the simulation result without using the experimental/numerical ***S*** parameters adjustments; the center image is the simulation result using the experimental/numerical ***S*** parameters adjustments. The right image is the experimental result.

1.Wald LL, Wiggins et.al. Applied Magnetic Resonance 2005;29(1):19-37.
2.Vaughan JT, Garwood M, et al. Magn Reson Med 2001;46(1):24-30.
3.Beck B, Plant DH, et al. Magma 2002;13(3):152-157.
4.Ibrahim TS, Lee R, et al..Magn Reson Imaging 2001;19(2):219-226.
5.Katscher U, Bornert P, et al. Magn Reson Med 2003;49(1):144-150.
6.Ibrahim TS, Lee R, et al. Magn Reson Imaging 2000;18(6):733-742.
7.Hoult DI, Kolansky G, et al. J Magn Reson 2004;171(1):64-70.
8.Wald L, Roell S, Fontius U, et al. 2006 May; Seattle. p 127.
9.Ibrahim TS, Abraham D, et al. 2006; Seattle, WA. ISMRM. p 1384.